



Neural Activity and Decoding of Action Observation Using Combined EEG and fNIRS Measurement

Sheng Ge¹, Peng Wang¹, Hui Liu¹, Pan Lin^{2,3}, Junfeng Gao³, Ruimin Wang⁴, Keiji Iramina⁴, Quan Zhang^{5*} and Wenming Zheng^{1*}

¹Key Laboratory of Child Development and Learning Science of Ministry of Education, School of Biological Science and Medical Engineering, Southeast University, Nanjing, China, ²Department of Psychology and Cognition and Human Behavior Key Laboratory of Hunan Province, Hunan Normal University, Changsha, China, ³College of Biomedical Engineering, South-Central University for Nationalities, Wuhan, China, ⁴Department of Graduate School of Systems Life Sciences, Kyushu University, Fukuoka, Japan, ⁵Neural Systems Group, Massachusetts General Hospital, Harvard Medical School, Charlestown, MA, United States

OPEN ACCESS

Edited by:

Mingzhou Ding,
University of Florida, United States

Reviewed by:

Yongtian He,
University of Houston, United States
Zhen Yuan,
University of Macau, China

*Correspondence:

Quan Zhang
qzhang@nmr.mgh.harvard.edu
Wenming Zheng
wenming_zheng@seu.edu.cn

Specialty section:

This article was submitted to
Cognitive Neuroscience, a section of
the journal *Frontiers in Human
Neuroscience*

Received: 08 December 2018

Accepted: 24 September 2019

Published: 15 October 2019

Citation:

Ge S, Wang P, Liu H, Lin P, Gao J,
Wang R, Iramina K, Zhang Q and
Zheng W (2019) Neural Activity and
Decoding of Action Observation
Using Combined EEG and fNIRS
Measurement.
Front. Hum. Neurosci. 13:357.
doi: 10.3389/fnhum.2019.00357

In a social world, observing the actions of others is fundamental to understanding what they are doing, as well as their intentions and feelings. Studies of the neural basis and decoding of action observation are important for understanding action-related processes and have implications for cognitive, social neuroscience, and human-machine interaction (HMI). In the current study, we first investigated temporal-spatial dynamics during action observation using a combined 64-channel electroencephalography (EEG) and 48-channel functional near-infrared spectroscopy (fNIRS) system. We measured brain activation while 16 healthy participants observed three action tasks: (1) grasping a cup with the intention of drinking; (2) grasping a cup with the intention of moving it; and (3) touching a cup with an unclear intention. The EEG and fNIRS source analysis results revealed the dynamic involvement of both the mirror neuron system (MNS) and the theory of mind (ToM)/mentalizing network during action observation. The source analysis results suggested that the extent to which these two systems were engaged was determined by the clarity of the intention of the observed action. Based on the difference in neural activity observed among different action-observation tasks in the first experiment, we conducted a second experiment to classify the neural processes underlying action observation using a feature classification method. We constructed complex brain networks based on the EEG and fNIRS data. Fusing features from both EEG and fNIRS complex brain networks resulted in a classification accuracy of 72.7% for the three action observation tasks. This study provides a theoretical and empirical basis for elucidating the neural mechanisms of action observation and intention understanding, and a feasible method for decoding the underlying neural processes.

Keywords: action observation, mirror neuron system, theory of mind, complex brain network, EEG, fNIRS

INTRODUCTION

Action observation is a cognitive process enabling understanding, choosing and imitating the form and motion of an action by observing the actions of another person (Lee et al., 2012). Observing the behavior of others and understanding their intentions is an essential component of social behavior. Action understanding and imitation of others' actions may help an observer understand

the intention and emotional state of the agent involved (Libero et al., 2014). Previous studies have indicated that action observation can improve motor performance (Gatti et al., 2013) and motor skill learning (Kim et al., 2017). Moreover, as a safe and easy therapy for clinical rehabilitation and treatment of stroke, Parkinson's disease and autism spectrum disorder, observing the actions of others has been reported to improve motor function (Harmsen et al., 2015; Caligiore et al., 2017) and facilitation of social interaction (Perkins et al., 2015). Observation and understanding the intention of action is a fundamental requirement for human-machine interaction (HMI). In HMI scenarios, action intention understanding between humans and machines is the basis of interaction. During these interactions, it is important to enable the machine to understand the human's action intention (Casalino et al., 2018). Previous studies have made substantial progress toward enabling machines to understand the action intention of humans (Hernandez et al., 2014; Foster et al., 2017; Bandara et al., 2018). Meanwhile, it is also crucial to construct a feedback route from the human to the machine, to let the machine know that the human has understood the intention of the machine's action during the interaction. For example, in a home care situation with HMI, a robot may have the intention to feed a user, while the user may not notice the action of the robot. In such a case, the robot should stop the action immediately to avoid a dangerous situation. However, research on this topic is currently lacking. Therefore, in the current study, we attempted to use brain signals as feedback signals for the machine, to make the machine aware of the human's process of intention recognition.

The mirror neuron system (MNS) is believed to underlie the human ability to understand others' actions and intentions during action observation, *via* a direct-matching process (Rizzolatti and Craighero, 2004; Kanakogi and Itakura, 2010), by which visuomotor information is transformed into motor knowledge (Jeon and Lee, 2018). The MNS provides a neural basis for recognizing the observed action. Consequently, action recognition involves the recognition of the goal of an action (i.e., action understanding; Rizzolatti et al., 2001; Iacoboni et al., 2005). The MNS responds maximally when observing object-directed interactions of a hand with an object (Rizzolatti et al., 2001) and hand-object interaction is a necessary condition to trigger the MNS (Umiltà et al., 2001). Intention understanding involves the integration of representations of the meaning and intent of the action based on hand-object interaction (Ortigue et al., 2009). The MNS mainly includes the premotor cortex (PMC), inferior frontal gyrus (IFG), superior parietal lobule (SPL), and rostral inferior parietal lobule (IPL; Molenberghs et al., 2012; Jeon and Lee, 2018).

Once others' actions are mapped onto the observer's own motor representation of the same action, the observer can understand the actions and predict the relationships between external states of affairs and internal states of mind, which leads to the activation of "theory of mind" (ToM; also referred to as mentalizing or mental state reasoning; Rizzolatti et al., 2001; Jeon and Lee, 2018). Unlike action observation, mental state reasoning requires high-level cognitive and attentional resources (Lin et al., 2010) and is believed to be unique to

humans (Call and Tomasello, 2008). Widely distributed neural networks have been consistently implicated in ToM, including the temporoparietal junction (TPJ), superior temporal sulcus (STS), posterior cingulate cortex/precuneus (PCC/PC), medial prefrontal cortex (MPFC), and anterior temporal lobes (ATL; Rilling et al., 2004; Yang et al., 2015).

As a classical neural imaging methodology, electroencephalography (EEG) provides a measure of the electrical potentials generated by cortical postsynaptic currents. EEG not only reflects the momentary activity of a population located near the recording electrodes but also distal populations *via* the volume conduction effect (He et al., 2011). EEG has the advantage of low-cost, safety, portability, and high temporal resolution, but is limited by electromagnetic and motion interference. Functional near-infrared spectroscopy (fNIRS) is an emerging non-invasive brain-imaging methodology using near-infrared light to monitor changes in the concentration of oxyhemoglobin (HbO), deoxyhemoglobin (HbR) and total hemoglobin (HbT = HbO + HbR) in the superficial layers of the cerebral cortex beneath a pair of source and detector optodes. Because of its low cost, safety, portability, and acceptable spatial resolution, fNIRS is increasingly used in research and clinical applications (Boas et al., 2014; Kamran et al., 2016). fNIRS relies on the relationship between local neural activity and changes in regional cerebral blood flow (rCBF) affecting oxygenation and hemoglobin content in blood vessels; local cortical activation causes an increase in HbO and HbT, with a corresponding decrease in HbR (Villringer and Chance, 1997). Compared with fMRI, fNIRS has important advantages for measurement in real-world situations, including a relative lack of constraints of the experimental environment, and the robustness of the signal against motion artifacts. These features enable fNIRS to expand the potential applications of measurement in real-world environments (Balardin et al., 2017).

EEG and fNIRS differ markedly in terms of the underlying imaging principles and physiological concepts. Because EEG and fNIRS each have specific limitations (e.g., low spatial resolution for EEG, and low temporal resolution for fNIRS), the advantages of combining EEG and fNIRS measurements could provide an approach for overcoming the limitations of each method. EEG-fNIRS measurement acquires brain activation from different physiological signals, which could increase data quality and quantity. Moreover, bimodal EEG-fNIRS could provide additional information about neurovascular coupling (NVC), which is the cascade of processes by which neural activity modulates local cerebral hemodynamic properties (Keles et al., 2016). EEG electrodes and fNIRS optodes have good adaptability in terms of spatial configuration. Finally, many studies have found that bimodal EEG-fNIRS signals provide more feature information than single-mode EEG or fNIRS systems, which can significantly improve classification accuracy (Hong and Khan, 2017; Khan and Hong, 2017). For these reasons, bimodal EEG-fNIRS measurement has substantial potential in research and practical applications (Fazli et al., 2012; Ahn and Jun, 2017; Berger et al., 2018). Because action observation is a dynamic and complex spatiotemporal process (Gardner et al., 2015; Ge et al., 2017), bimodal EEG-fNIRS measurement has important

advantages for exploring its dynamic processes in terms of both temporal and spatial characteristics. To the best of our knowledge, aside from previous studies in our laboratory (Zhang et al., 2015; Ge et al., 2017), no action observation studies using EEG-fNIRS bimodal measurement have been reported.

Recently, complex brain network-based graph theoretical analysis has become a powerful and popular approach for analyzing brain imaging data (Yu et al., 2018). Complex brain networks can reveal the mechanisms and characteristics of brain structure and function that cannot be discovered by past analytical methods, such as modularity, hierarchy, centrality, and the distribution of network hubs (Bullmore and Sporns, 2009). The complex brain network is a powerful approach to identify the similarities and differences of brain activation in many applications, such as brain-computer interface classification (Zhang et al., 2016), mental illness diagnosis (Fang et al., 2017; Shon et al., 2018), fatigue detection (Han et al., 2019), and emotional cognitive classification (Liang et al., 2018). However, to date, few studies have used complex brain networks to classify action observation and understanding. Consequently, exploring the whole-brain complex brain network patterns during the observation and understanding of different action intentions would be meaningful.

The current study sought to investigate the neural basis of action observation and to classify the action observation process based on brain signals. To this end, we first used bimodal EEG-fNIRS measurement to investigate temporal-spatial dynamics during action observation. We then constructed complex brain networks based on EEG and fNIRS data to classify the brain activity corresponding to action observation with different intentions. We expected that the brain activation analysis method based on EEG-fNIRS bimodal signals in the current study would extend understanding of the spatiotemporal features of the neural mechanisms underlying action intention understanding. In addition, the intention classification method in the current study could provide a new research direction for human-computer interaction research.

MATERIALS AND METHODS

Participants

Sixteen healthy adults [six females and 10 males; mean age = 24.1 years, standard deviation (SD) = 1.3, range 22–26 years] participated in the study. None of the participants reported a history of neurological conditions or psychosis, or used medication. All participants had normal or corrected-to-normal vision and were confirmed to be right-handed using the Edinburgh Handedness Inventory. All participants provided written informed consent in accordance with the Declaration of Helsinki (World Medical Association, 2013) before enrolment in the study, which was approved by The Ethics Committee of Affiliated Zhongda Hospital, Southeast University (2016ZDSYLL002.0 and 2016ZDSYLL002-Y01). Each participant received 200 RMB for participating, after the experiment.

Before recording, participants were informed that some of the hand-cup interaction stimuli without context may be associated

with the following intentions: (1) grasping a cup with the intention of drinking; (2) grasping a cup with the intention of moving it; and (3) touching a cup with an unclear intention. All participants were familiarized with each of the actions in a 3.2 min training session. After the session, participants were debriefed to ensure they understood the experimental instructions and correctly understood the action intentions shown. During EEG-fNIRS measurement, participants received clear instructions to carefully observe the three different kinds of hand-object interaction stimuli and attempt to understand the intention behind the stimuli. There is no behavioral response required from participants. To avoid eye and muscle movement interference, participants were asked to look at the cross at the center of screen and to make no verbal responses throughout the experiment.

Experimental Procedure

There were three kinds of hand-cup interaction stimuli (**Figure 1**, partially referring to Ortigue et al., 2010) corresponding to different potential intentions: (a) A right hand grasping the handle of the cup with the intention to drink from it (Sd); (b) a right hand grasping the rim of a cup with the intention to move it (Sm); and (c) a right hand touching the rim of a cup without a clear intention (Su). Participants were seated in a comfortable chair in a dark shielded room with their heads placed on a chin-rest (**Figure 2**). The stimuli were displayed on a computer monitor 80 cm away from the participants. The size of the stimuli was H: 28 cm (19.85° of visual angle) × V: 16 cm (11.42° of visual angle).

Figure 3 shows a schematic diagram of the bimodal EEG-fNIRS measurement procedure used in the current study. The visual stimuli were programmed in E-Prime (Version 2.0, Psychology Software Tools Inc., Sharpsburg, PA, USA). Every trial included the following sequence. First, participants underwent a pre-rest period in which a fixation cross was presented for 6 s. This was followed by a preparation period, in which a cup appeared as a cue on the screen for 0.5 s, notifying the participant to prepare for the upcoming observation period. Then, in the observation period, a hand-cup interaction stimulus was presented for 3.5 s. Since the temporal interval between the preparation and observation periods was very short, a continuous image sequence could generate the perception of an action (Brown et al., 2010; Ortigue et al., 2010). During the observation period, participants were instructed to try to understand the intention corresponding to each observed stimulus. For convenience, the starting moment of observation period was defined as 0 time point. Finally, there was a post-rest period, in which participants rested for 6 s. The post-rest and pre-rest of two subsequent trials were used as the baseline period. To avoid an adaptation effect, the three hand-cup interaction conditions were presented in a random sequence. The color of the cup alternated randomly among seven colors, and each color was shown four times in the whole experiment. The whole experiment for each participant consisted of a total of 84 trials (three hand-cup interaction conditions × seven colors × four times) and divided into four equal sessions lasting for 28.4 min.



FIGURE 1 | Three kinds of hand-cup interaction stimuli corresponding to different potential intentions. **(A)** a right hand grasping the handle of the cup with the intention to drink from it (Sd); **(B)** a right hand grasping the rim of a cup with the intention to move it (Sm); **(C)** a right hand touching the rim of a cup without a clear intention (Su).



FIGURE 2 | Experimental environment.

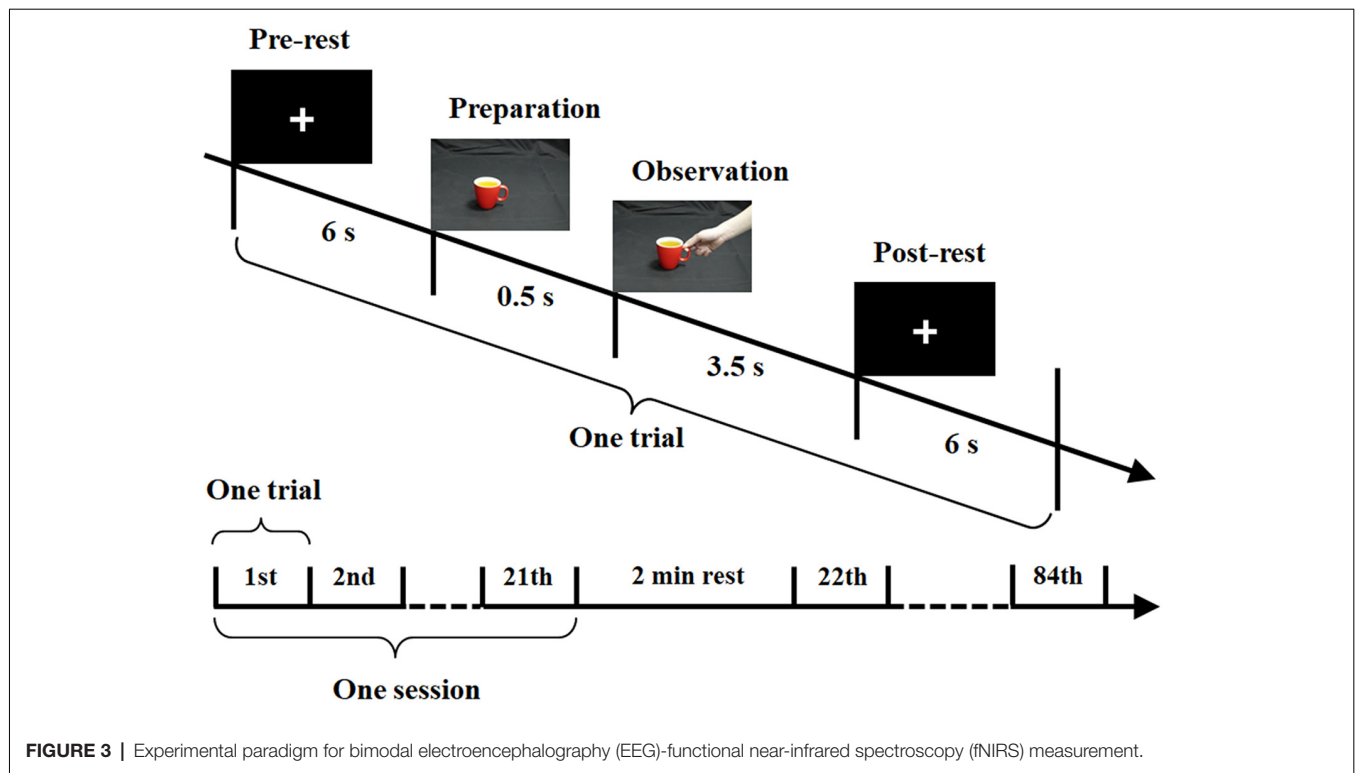
Each session was composed of 21 trials, with a 2-min rest between sessions.

Data Acquisition and Pre-processing

The current study used a 64-channel EEG and 48-channel fNIRS bimodal signals with simultaneous measurement (**Figure 4**). EEG signals were recorded with a Synamps2 EEG system (Neuroscan Synamps amplifier; Scan 4.5 Compumedics Corp., TX, USA) according to the international 10–20 system of electrode placement (**Figure 4A**). The reference electrode was placed on the left mastoid. Bipolar horizontal and vertical electrooculogram (EOG) derivations were recorded *via* two pairs of electrodes placed near the eyes. All electrode impedances were kept below 5 k Ω . EEG was recorded with a sampling frequency of 1,000 Hz and band-limited from 0.05 to 100 Hz, and

a notch filter was used to suppress powerline interference. An independent component analysis (ICA) based on EEG and EOG was performed to remove eye movement and blink artifacts (see Ge et al., 2017 for details). During the data analysis, EEG signals were pre-processed with a bandpass filtered between 1 and 30 Hz. EEG data for each trial were corrected by subtracting the average of the data points between -700 ms and -500 ms.

The fNIRS signals recording were recorded with a LABNIRS system (Shimadzu Company Limited, Kyoto, Japan). The absorption of three wavelengths (780, 805 and 830 nm) of continuous near infrared light was measured with a sampling interval of 27 ms, then transformed into concentration changes of HbO, HbR and HbT by the modified Beer-Lambert law (Delpy et al., 1988). fNIRS optodes were positioned over the 64-channel EEG cap (Neuroscan, Charlotte, NC, USA) and the optodes and



the electrodes were placed at intervals with a distance between the emitters and detectors of approximately 3 cm (Boas et al., 2004). We used a 48-channel system with 32 optodes (consisting of 16 emitters and 16 detectors) placed above the bilateral parietal areas. Channels 13 and 36 were set above the C3 and C4 areas, respectively (Figure 4B). In the current study, the locations of the optodes were measured using a 3D digitizer (FASTRAK; Polhemus, VT, USA). The fNIRS signals were pre-processed and bandpass filtered between 0.01 and 0.1 Hz. The fNIRS data for each trial were baseline-corrected by subtracting the average of the data points between -6.5 s to -0.5 s before observation period onset.

Sensor-Level Analysis

The averaged event-related potential (ERP) and HbO waveforms of all channels for all participants were analyzed, respectively to investigate time series characteristics. In addition, a *t*-test of the HbO signal between the observation and baseline block of each channel was conducted from 1 to 5 s with 1-s steps to investigate the characteristics of fNIRS signals over time. Based on this analysis, the topographical maps of the *t*-test results of HbO concentration over the bilateral parietal areas were obtained using an interpolation method (using the `griddata.m` function of MATLAB 2013a, The MathWorks, Natick, MA, USA).

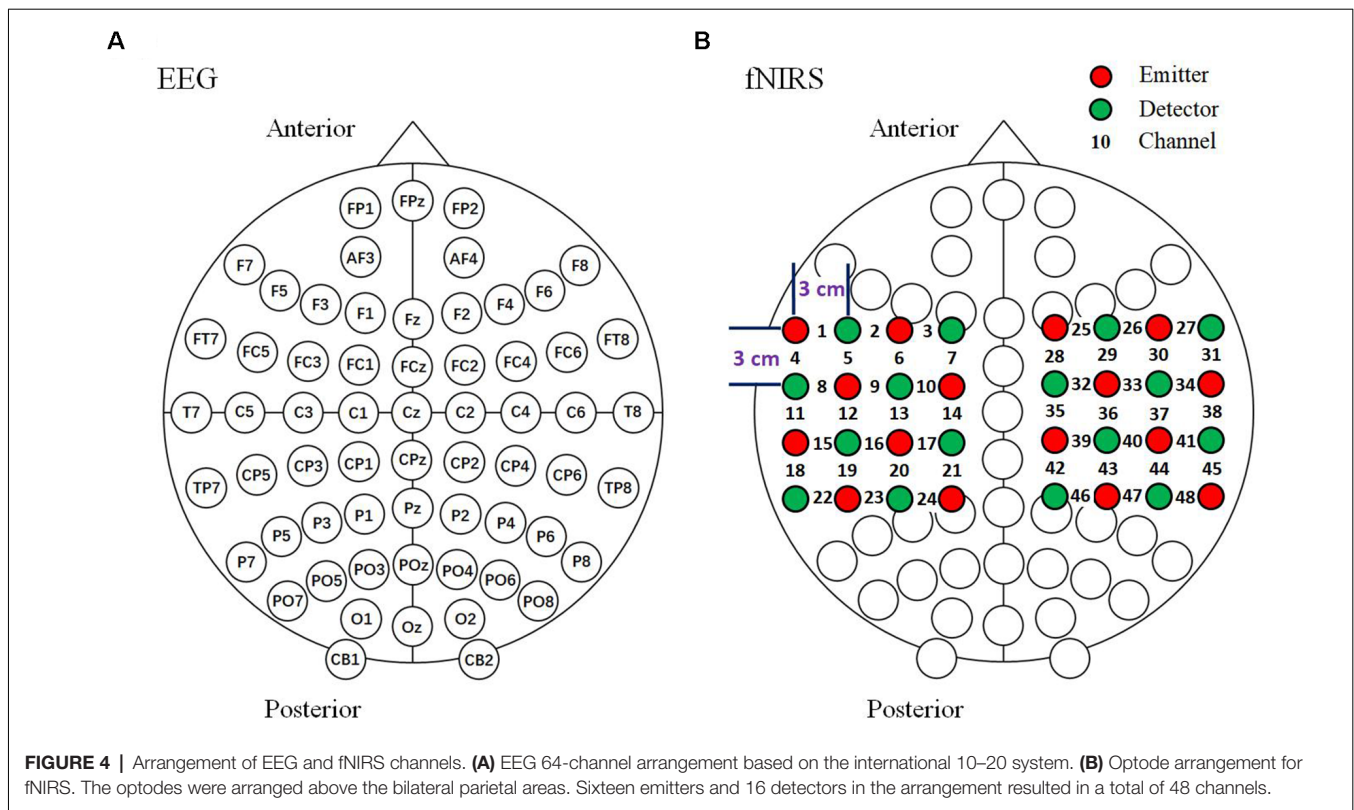
Source-Level Analysis

For EEG source analysis, the grand average for 16 participants was first calculated with MATLAB. Next, the standardized

low resolution electrical tomographic analysis (sLORETA)¹, a functional imaging method based on electrophysiological and neuroanatomical constraints (Pascual-Marqui, 2002) was applied to the 16-participant grand average. sLORETA estimates the intracerebral electrical sources by calculating the scalp current source density (CSD) based on EEG signals (Pascual-Marqui et al., 2002). The sLORETA method has relatively good accuracy for source localization, even for deep sources (Keeser et al., 2011) and the average localization error is less than one grid unit (Pascual-Marqui, 2002). The sLORETA algorithm calculates the standardized CSD values at each of the 6,239 voxels of cortical gray matter, hippocampus, and amygdala at 5 mm spatial resolution in the digitized Montreal Neurological Institute (MNI) coordinates, corrected to Talairach coordinates (Talairach and Tournoux, 1988). This calculation of the standardized CSD is based upon a linear weighted sum of scalp electric potentials. The sLORETA algorithm solves the inverse problem by assuming that the neighboring neuronal sources have related dipole orientations and amplitudes (represented by adjacent voxels; Pascual-Marqui, 2002).

For fNIRS source analysis, the 3D coordinates of the anatomical markers (i.e., the nasion, inion, Cz, and left and right preauricular points) and fNIRS optodes (16 emitters, 16 detectors) were first digitized using the FASTRAK digitizer (Polhemus, Colchester, VT, USA). Meanwhile, the coordinates of the midpoints between each pair of the emitters and detectors were automatically calculated as the coordinates of the fNIRS

¹<http://www.uzh.ch/keyinst/loreta.htm>



channel. Second, the spatial registration was implemented between each fNIRS channel and *t*-test topographical maps. Third, the *t*-test topographical maps were superposed onto the surface of the MNI standard 3D head model using FUSION 3D imaging software (Shimadzu Co., Ltd.).

Intention Classification Based on Complex Brain Network

For graph theoretical analysis, the complex brain network (Bullmore and Sporns, 2009) method is an emerging approach that can be applied to both anatomical and functional brain networks (Sporns, 2013). In the current study, we classified three different action intentions *via* complex brain networks based on EEG and fNIRS signals. First, we constructed two complex brain networks for EEG and fNIRS training datasets by treating EEG and fNIRS channels as nodes separately and determining their connections according to the Pearson's correlation coefficient between each pair of channels. Second, five nodal features (i.e., nodal network properties), including the degree (the number of neighbors connecting to a node), clustering coefficient (the degree to which nodes in the network tend to cluster together), betweenness centrality (the proportion of the shortest paths pass through a node), eigenvector centrality (the degree of a node correlates with other nodes that are themselves central within the network) and local efficiency (how well information is exchanged by a node's neighbors when it is removed) were calculated for EEG and fNIRS networks separately, according to the method reported in previous studies

(Santiago et al., 2016; Fang et al., 2017; Zhao et al., 2017). Third, we combined the nodal features of EEG and fNIRS networks together, and selected the features based on the Relief-F algorithm (Kononenko, 1994), scoring the features based on the identification of feature value differences between nearest neighbor instance pairs using the *relieff.m* function of MATLAB with the nearest neighbors $k = 10$. Fourth, we used the programming library LIBSVM (C-supporting vector classification; Chang and Lin, 2011) for support vector machine (Yu et al., 2006) as the classifier. The grid search algorithm was employed to find the optimal values of the kernel parameter γ and penalty factor C (Ge et al., 2014). Finally, the classification accuracy was obtained using the averaged accuracies of 10 times 10-fold cross-validation (25 and three trials for training and testing, respectively).

RESULTS

The averaged ERP waveforms of all channels for Sd, Sm and Su intentions for all participants are shown in **Figure 5** and **Supplementary Figure S1**. Statistical analysis was performed with one-way analysis of variance (ANOVA) and a Bonferroni test for the multiple comparisons procedure was performed as a *post hoc* analysis (IBM SPSS version 21.0). The statistical results revealed a statistically significant difference in the mean amplitude of ERPs during 350–400 ms for the three intentions at 43 channels (see channels marked with two asterisks in

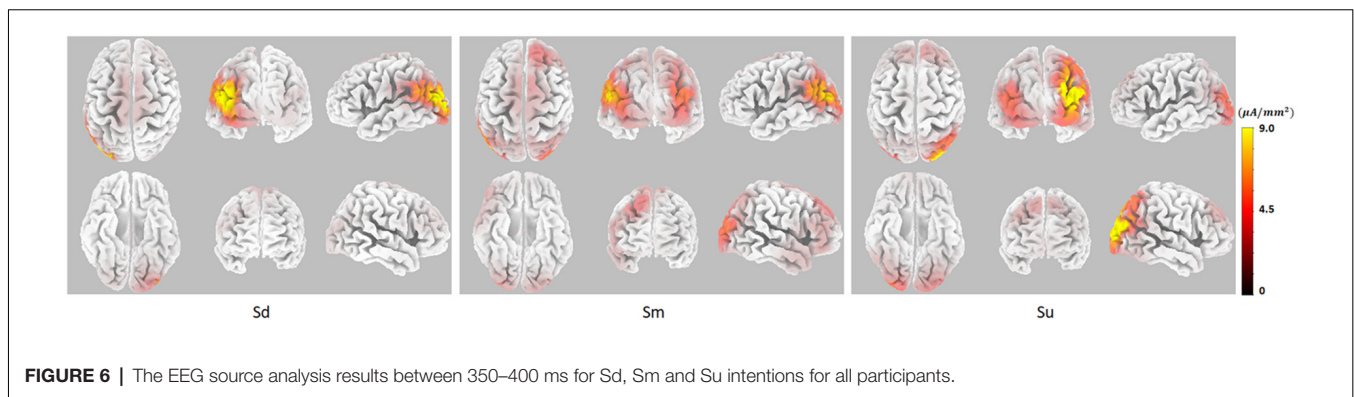
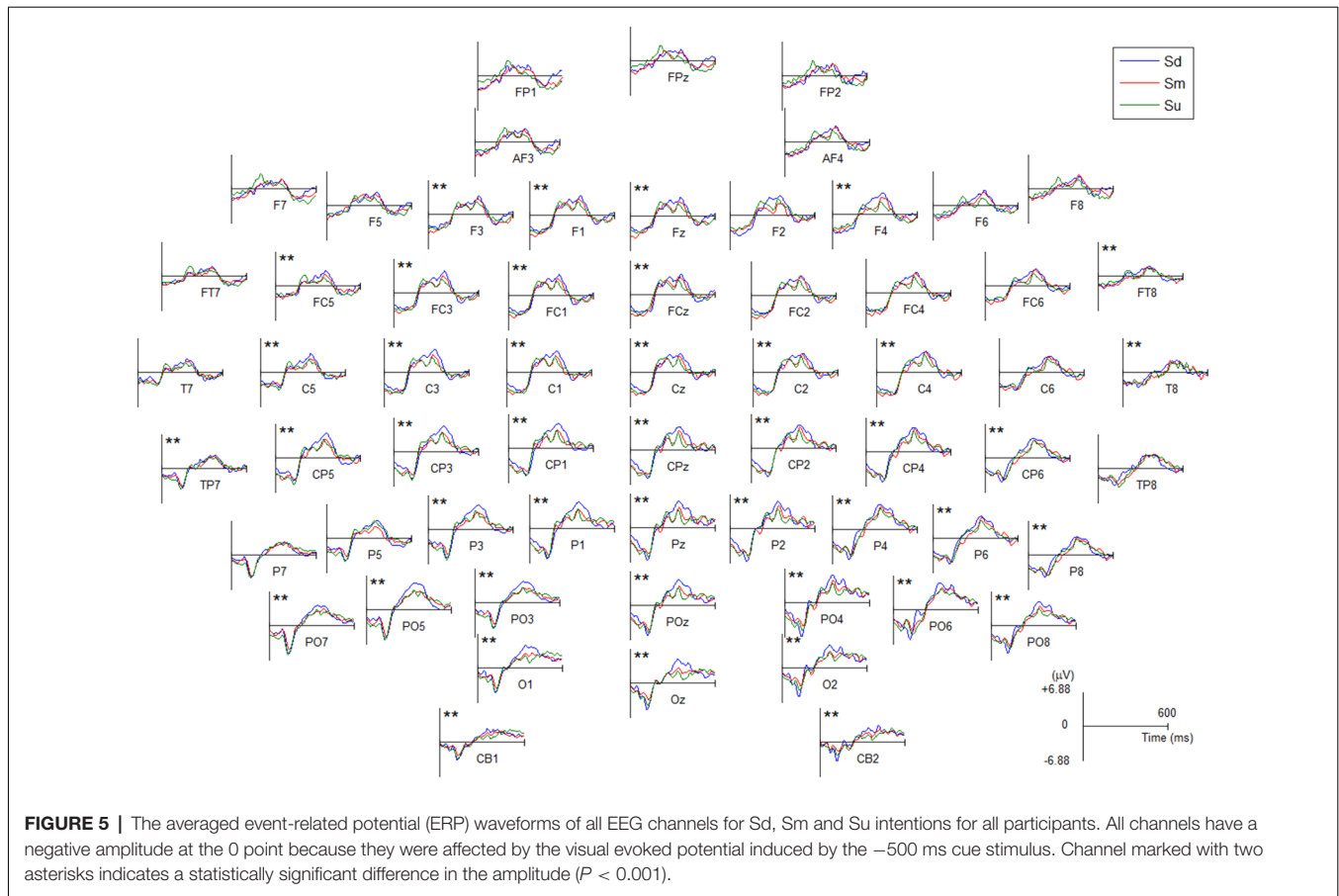


Figure 5, among these 43 channels the lowest $F_{(2,150)} = 50.7$, $P < 0.001$). Moreover, the *post hoc* tests showed that among these 43 channels, Sd had a significantly greater amplitude than Sm and Su (highest $P < 0.001$, Bonferroni-corrected, respectively), while Sm had a significantly greater amplitude than Su (highest $P < 0.001$, Bonferroni-corrected).

EEG source analysis was implemented for the three intentions between 350–400 ms, revealing that, stable and identical activation regions were found during 350–400 ms, the Sd task mainly induced activation in the left hemisphere, including the

middle occipital gyrus (MOG; BA18, 19), superior occipital gyrus (SOG; BA19), middle temporal gyrus (MTG; BA19, 39), superior temporal gyrus (STG; BA39), and angular gyrus (AG; BA39). The Sm task also induced activation that was mainly located in the left hemisphere, including the same activation areas, although this activation was weaker. In contrast, Su mainly induced right hemisphere activation, including the MOG (BA19), SOG (BA19), cuneus (BA19), MTG (BA19, 39), AG (BA39) and SPL (BA 7). The source analysis results between 350–400 ms are shown in **Figure 6**.

The grand averaged HbO waveforms of fNIRS for three intentions are shown in **Figure 7** and **Supplementary Figure S2**. The same ANOVA process used for grand averaged ERPs, as described in the previous paragraph, was used to analyze the difference of HbO waveforms among three intentions. The ANOVA statistical results revealed a statistically significant difference in the mean amplitude of HbO during 0–3.5 s for the three intentions at 11 channels (see channels marked with an asterisk in **Figure 7**, among these 11 channels the lowest $F_{(2,387)} = 16.5$, $P < 0.05$). Moreover, the *post hoc* tests showed that there are statistically significant differences between pairwise contrasts of the three conditions among these 11 channels (highest $P < 0.05$, Bonferroni-corrected). However, the differences were not identical in the three conditions among these 11 channels.

Topographical maps of *t*-test results of the HbO signal between the observation and baseline block of each channel from 1 to 5 s for all participants are shown in **Figure 8**. A peak value can be clearly seen at 3 s. For this reason, we implemented fNIRS source analysis at 3 s. The results are shown in **Figure 9**. The results in **Figure 9** indicate strong activations in the bilateral PMC, IFG, and TPJ for all three conditions, while activation in the left hemisphere was stronger than that in the right hemisphere. The *t*-values of the topographical map revealed that activation intensity exhibited a pattern of $S_d > S_m > S_u$.

In this study, we used a cross-correlation calculation method (Pfurtscheller et al., 2012; Sood et al., 2016) to compute the correlation between grand averaged ERP and HbO waveforms. For 0–X ms EEG data [$X \in (100\ 600)$ ms, in steps of 1 ms], an equal length fNIRS data was selected and lagged Y ms behind EEG [$Y \in (0\ 3,000)$ ms, in steps of 27 ms]. The correlation coefficients between ERP and HbO data for three different conditions (S_d , S_m and S_u) were calculated, corresponding to every combination of X and Y. Areas with correlation coefficients greater than 0.8 for all three conditions (S_d , S_m and S_u) were plotted with contour lines in **Figure 10**. The correlation analysis indicated a strong correlation between EEG and fNIRS when the length of the EEG and fNIRS recording was approximately 385 ms, and the fNIRS signal was around 1700 ms behind the EEG signal.

The complex brain networks for the 0–3.5 s observation period of the EEG and fNIRS grand averaged datasets were calculated, respectively by treating channels as nodes, and determining the connections according to the Pearson's correlation coefficient between each pair of channels, and normalizing these values to Fisher's Z-values. A typical example of complex brain networks in the EEG and fNIRS datasets (participant No. 10) is shown in **Figure 11**. In this figure, a clear distinction can be seen between the complex networks of the three intentions.

The averaged classification results for three intentions of each participant based on the five features of complex brain networks calculated from EEG, fNIRS and EEG-fNIRS signals are shown in **Table 1**. The ANOVA results revealed a strong significant difference between three action observation tasks ($F_{(2,45)} = 39.12$, $P < 0.001$). In addition, EEG-fNIRS and EEG had significantly higher accuracy than fNIRS ($P < 0.001$, Bonferroni-corrected, respectively). Although the accuracy of EEG-fNIRS was higher

than EEG, there was no significant difference between this two modes ($P = 0.28$, Bonferroni-corrected).

The averaged confusion matrices for EEG, fNIRS and EEG-fNIRS classifications for all participants are shown in **Figure 12**.

DISCUSSION

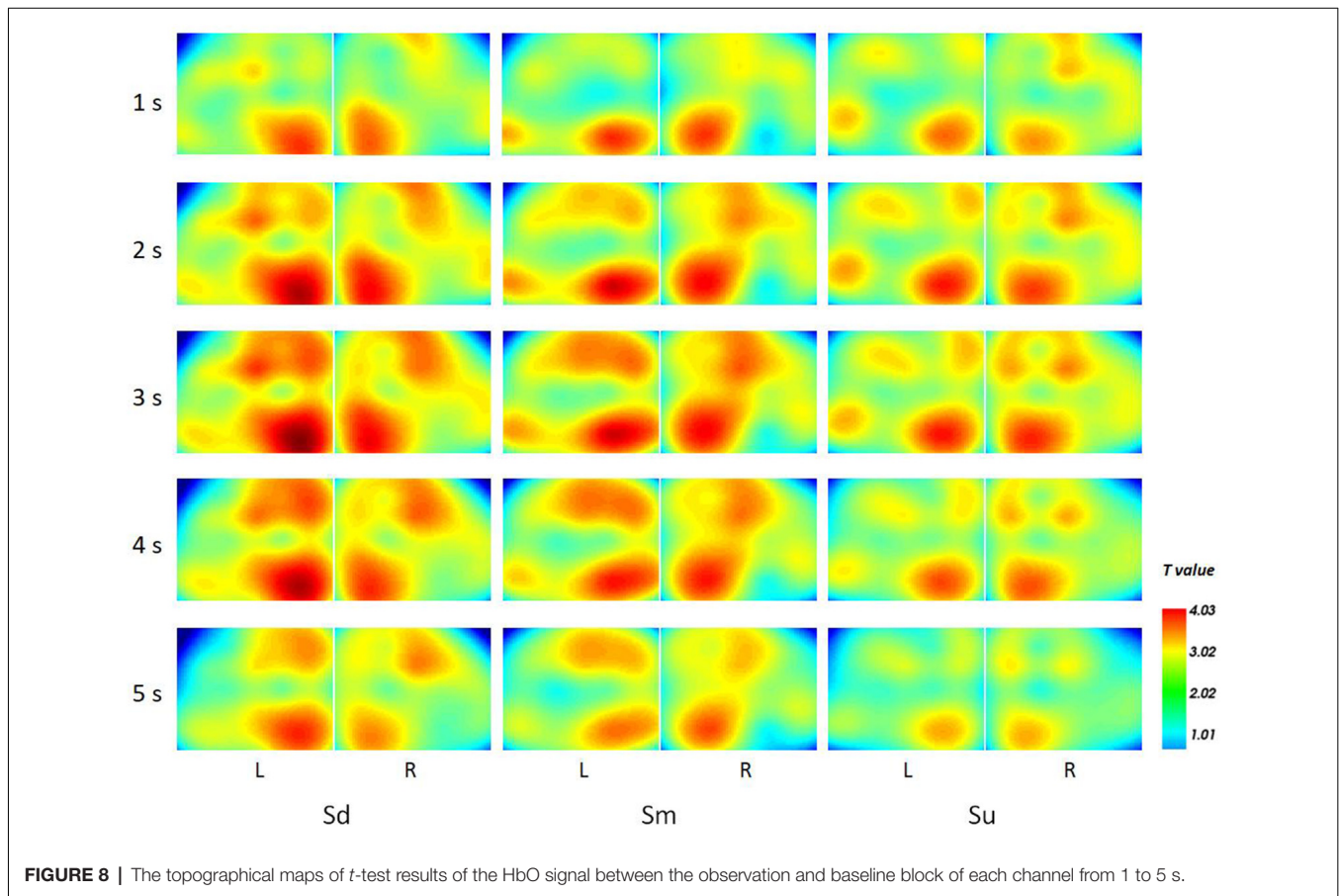
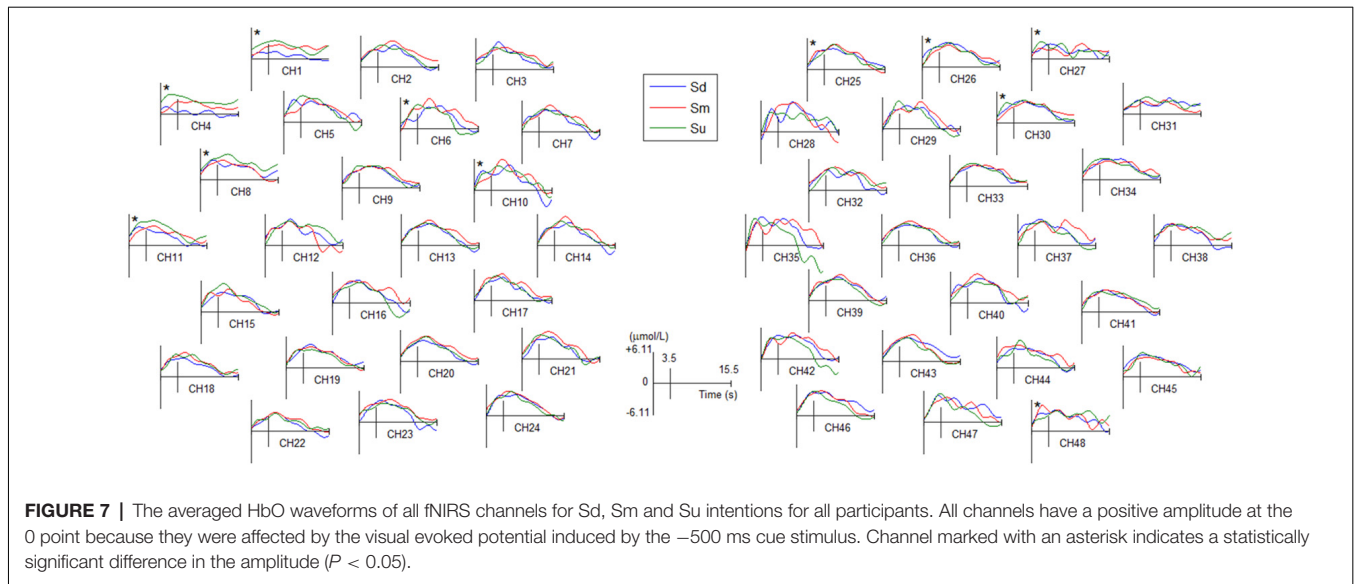
In the current study, we found particularly strong activation in the AG, which is the main part of the IPL. This finding is consistent with previous human neuroimaging studies identifying the IPL as a key region for the coding of intention. This structure is part of a frontoparietal system that links observed and stored actions through direct matching (Rizzolatti et al., 2014) in terms of the actions themselves (Iacoboni, 2009) or goals (Hamilton, 2015). In addition, Reader et al.'s (2018) findings indicated that the IPL plays a role in kinematic processing of actions, regardless of whether they are meaningful or meaningless, which provides direct support for the current results.

The SPL has previously been reported to be activated during both action observation and execution (Rizzolatti et al., 2014) and is considered to play a critical role in mental rotation and spatial transformation (Buneo and Andersen, 2006; Lamm et al., 2007). Oh et al.'s (2019) model indicated that the SPL may be involved in visuospatial transformation, allowing the MNS to observe and imitate actions independently of demonstrator-imitator spatial relationships.

In accordance with Jelsone-Swain et al.'s (2015) findings, we observed activity in the MTG for all three task conditions. Accordingly, Kilner identified the MTG as the primary region bridging the two neural pathways involved specifically in action understanding (Kilner, 2011).

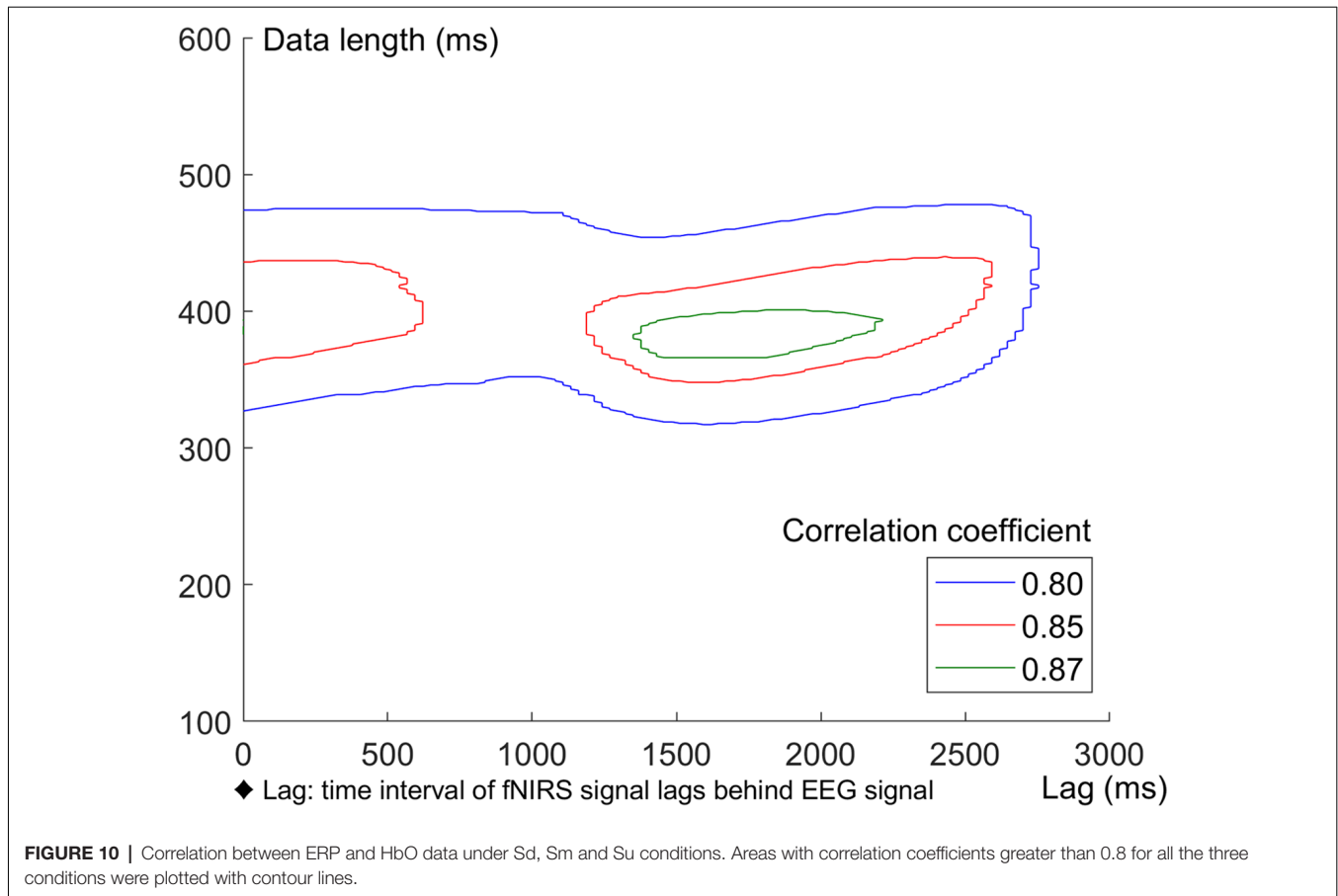
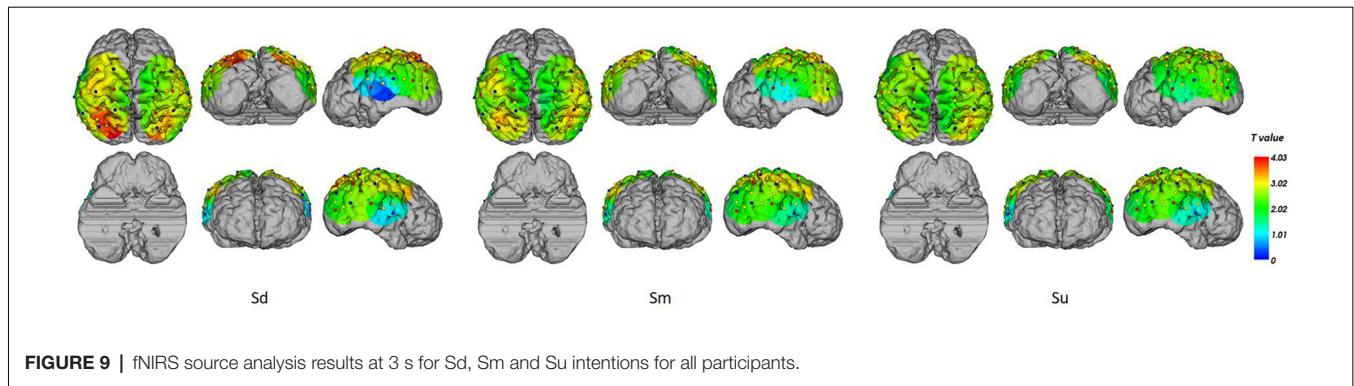
The current results revealed activation in primary visual regions including the MOG, SOG and cuneus for all three intention conditions. STG activation was observed in both the S_d and S_m tasks. The STG is a higher-order visual region and has been reported to play key roles in the identification of goal-directed movements (Schultz et al., 2004) and observation of biological motion (Matthys et al., 2009).

Previous studies using similar tasks reported that the mirror function of the brain is increased when the observed actions are familiar and have clear intentions (as in the “grasping a cup for drinking” and “grasping a cup for moving” conditions). In contrast, in the “touching a cup without clear intention” condition, the mirror function of the brain would be expected to be suppressed because the perceived action is outside the observer's repertoire of familiar movements, which induces a lower level of activity (de Lange et al., 2008; Ge et al., 2017; Zhang et al., 2018). This tendency was observed in the current study, indicating that, during familiar action observation (S_d and S_m tasks), the processing of motor information leading to goal understanding (direct-matching process) requires more effort because of the complexity of the observed grip and its relationship with the object. However, such a process does not occur in the case of unfamiliar actions (S_u), in which a less direct matching process is implemented.



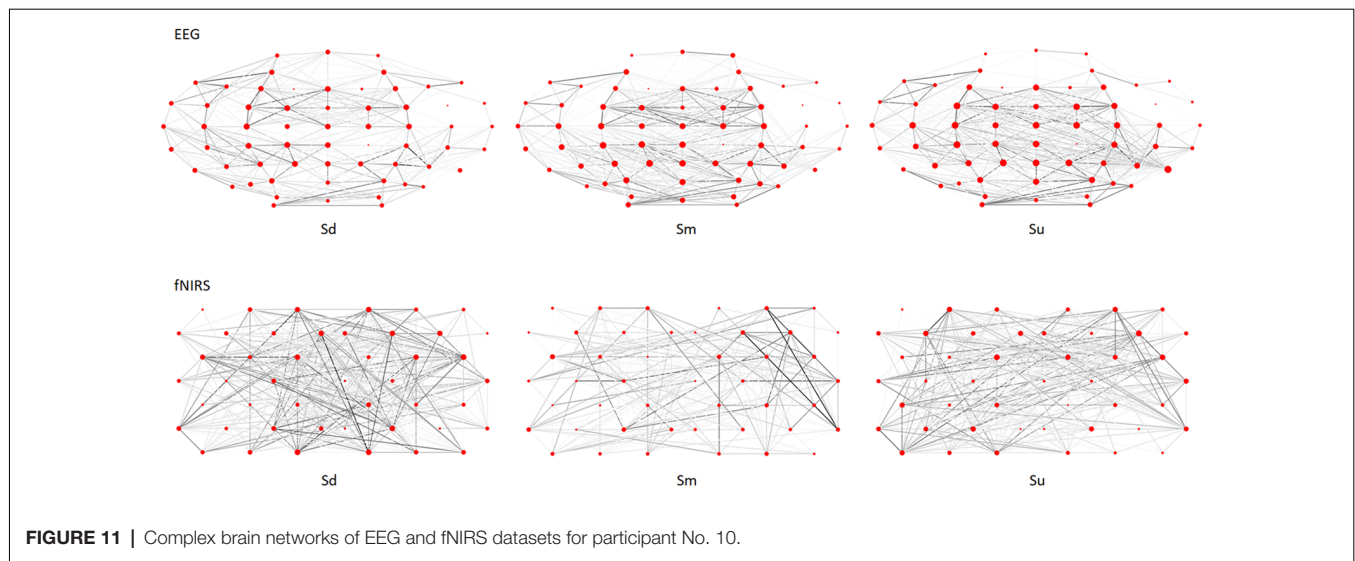
Several previous studies concluded that the MNS network is active during the visual processing of others' actions (how and what), while the ToM network is additionally recruited to process their intentions (why; de Lange et al., 2008; Spunt

et al., 2010). In a recent review, Eren proposed that MNS and ToM functions are more complex than traditionally thought, with interrelated rather than independent functions (Eren, 2009). Based on Rizzolatti et al.'s (2014) definition, understanding the



goal of a motor act performed by another individual involves two levels of insight: first, understanding of “what” the other is doing (e.g., grasping a cup); second, the understanding of “why” the other is doing it, which is considered the action overarching intention (e.g., grasping a cup for drinking). Previous studies have indicated that in low-level action understanding, the MNS obtains direct awareness of the goal of an action by recognizing what an action is and how it is being performed, particularly for familiar or frequently executed actions, whereas at a higher level of action understanding, the MNS might respond to why an action is being performed (Thioux et al., 2008; van Overwalle and

Baetens, 2009). Many previous studies of action understanding suggested that the left hemisphere MNS is primarily related to the encoding of the motor act itself (what). In contrast, the right hemisphere MNS may be involved in the process of understanding the intentions underlying the actions (why; Ortigue et al., 2010; Ge et al., 2017). Some studies have proposed that, in the absence of context information or when observing unusual actions, the ToM network might be particularly strongly recruited to supplement insufficient information by inferring others’ mental states (de Lange et al., 2008; Spunt et al., 2011). In the current study, we found clear activation shifts



from the left to the right hemisphere when changing from observing familiar actions with clear intentions (Sd and Sm tasks) to observing unfamiliar actions without a clear intention (Su task). This finding is in accord with previous studies by Ortigue et al. (2010), Ge et al. (2017) and Zhang et al. (2018). We assumed that when an action was more familiar or clear, direct-matching processing in the left hemisphere would be more strongly engaged. In contrast, we assumed that a more novel or ambiguous action would engage more inferential or mentalizing processes in the right hemisphere. The current results support the notion that observing the actions of people with clear intentions recruits the MNS, enabling an immediate understanding of the observed acts and of the agent's intentions. However, when actions without clear intentions are observed, inferential or mentalizing processes based on the ToM appear to be engaged (Ge et al., 2017). Thus, our findings indicate that information processing during action observation is a complex process that cannot be attributed to a single neuronal mechanism.

Bimodal EEG-fNIRS measurement provides an approach to investigate brain activation with different spatial and temporal resolutions. EEG measures functional brain activity directly by detecting variations in electrical activity, which is a rapidly changing signal. In contrast, fNIRS measures functional brain activity indirectly *via* changes in the concentration of oxygenated and deoxygenated hemoglobin, which is a slowly changing signal. Previous ERP studies reported early mirror neuron activation of the P1, N170 and N400 components (Mohring et al., 2014), while the ToM or mentalizing network exhibited activation of the late negative ERP component at approximately 300–1,100 ms (Beudt and Jacobsen, 2015). The ERP waveforms revealed that mirror neuron ERP components oscillated between positive and negative components in a short time period, while the ToM or mentalizing network activation exhibited a long-term stable ERP component. Thus, the EEG source analysis in the current study may have reflected rapidly changing mirror neuron activation, while fNIRS source analysis may have reflected

slowly changing activation of the ToM or mentalizing network. Because EEG and fNIRS have different imaging mechanisms and measure different physiological signals, the bimodal EEG-fNIRS measurement used in the current study may provide more complete biological information with different spatial and temporal resolutions (Putze et al., 2014). Thus, this combined method could enable more comprehensive knowledge of action observation and understanding.

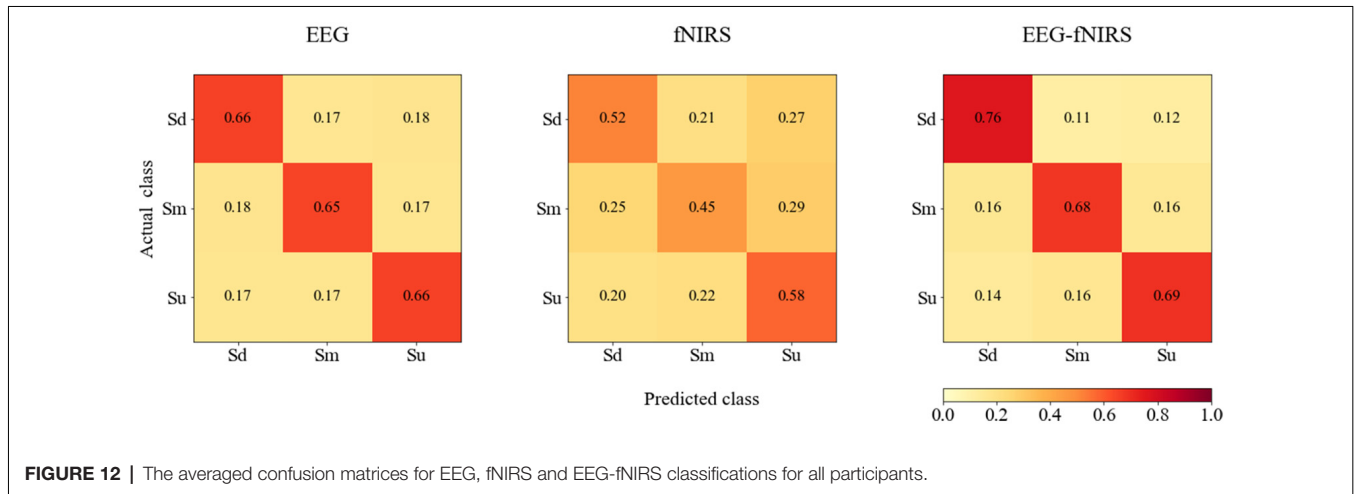
In addition, bimodal EEG-fNIRS measurement can quantitatively study the NVC (Govindan et al., 2016), reflecting the mechanism linking transient neural activity to subsequent changes in CBF. A high temporal and spatial correlation exists between neuronal activity and CBF [i.e., brain regions with high activity exhibit an accompanying increase in the amount of blood flow (Hendriks et al., 2019)]. In the current study, we also investigated the NVC between EEG and fNIRS signals and found a high correlation between these signals. This result was consistent with previous reports (Girouard and Iadecola, 2006; Govindan et al., 2016), indicating that neural activity is closely related to CBF. The correlation analysis between the grand averaged ERPs and HbO waveforms revealed a high correlation between EEG and fNIRS when the EEG and fNIRS length was approximately 385 ms (starting from 0 ms) and the fNIRS signal lagged approximately 1,700 ms behind the EEG signal. These results demonstrate the lag of the fNIRS signal behind the EEG signal and help to elucidate the temporal features of NVC corresponding to action intention understanding.

As we discussed in the preceding three paragraphs, the findings of previous studies and the current study indicated distinct differences in the timing and location of activation in response to different types of action intention observation. Such temporal and spatial dynamics of cortical activity can cause different topological characteristics of complex brain networks corresponding to observations of different types of action intentions (e.g., **Figure 11**), enabling the possibility of intention classification. Specifically, the current results

TABLE 1 | The classification results for three intentions of each participant based on the five features of complex brain networks calculated from electroencephalography (EEG), functional near-infrared spectroscopy (fNIRS) and EEG-fNIRS signals.

Accuracy (%)	S1	S2	S3	S4	S5	S6	S7	S8	S9	S10	S11	S12	S13	S14	S15	S16	Avg	SD
EEG	65.1	68.9	80.2	60.2	82.5	73.3	76.4	63.3	69.9	56.9	64.6	71.6	62.6	68.2	70.4	63.7	68.6	6.8
fNIRS	56.3	61.4	51.8	53.2	55.2	57.2	50.1	48.0	55.1	59.0	54.7	70.1	50.4	37.7	44.3	38.9	52.7	7.9
EEG-fNIRS	73.4	70.2	79.5	65.9	80.1	71.5	81.2	74.3	75.1	73.5	67.1	73.0	68.3	69.4	68.9	72.3	72.7	4.4

Avg: average; SD: standard deviation.



indicated that three types of complex brain networks exist, each corresponding to the observation of different action intentions. Because different action intention observations cause differences in cortical activation, the topological characteristics of the three complex brain networks appear to be different. In the current study, we used complex brain networks to classify different types of action observations based on bimodal EEG-fNIRS signals. **Table 1** reveals that the classification accuracy of EEG-fNIRS was 72.7%, which was higher than that of EEG or fNIRS alone. In addition, single-mode EEG achieved better performance than fNIRS (68.6% vs. 52.7%). This finding indicated that EEG provided more distinguishable complex network features than fNIRS for some participants. In addition, the results revealed that the fNIRS accuracy was very low for some participants, which reduced the corresponding EEG-fNIRS accuracy compared with the single-mode EEG accuracy for those participants. This finding suggests the possibility that future studies may be able to improve feature extraction and selection for fNIRS signals. Despite these limitations, the current study demonstrated that complex brain networks based on bimodal EEG-fNIRS provide a powerful classification method for action observation classification, which may have useful applications in HMI.

In addition, according to **Figure 12**, bimodal EEG-fNIRS achieved better classification performance than single-mode EEG and fNIRS, while fNIRS exhibited the worst performance. For EEG, no classification difference was observed among the three classes. For fNIRS, the Sm class was most often misclassified. For EEG-fNIRS, the Sd class exhibited higher classification

accuracy than the Sm and Su classes. These results suggest that although single-mode fNIRS achieved intermediate classification performance, bimodal EEG-fNIRS signals could further improve classification performance. These findings suggest the possibility that further studies examining feature extraction and selection for fNIRS signals may be able to improve the classification performance of bimodal fNIRS and EEG-fNIRS systems.

CONCLUSION

To investigate the neural basis of action observation and understanding, we used bimodal EEG-fNIRS measurement to investigate the sensor- and source-level activations for action observation. The results indicated that information processing during action observation is a complex process involving the MNS and ToM networks. In addition, we tested a proposed method using complex brain networks to classify the brain activations for different action observation tasks. By combining the features of EEG and fNIRS complex brain networks, the method achieved a satisfactory classification accuracy (72.7%), demonstrating the possibility of encoding action observation and understanding.

ETHICS STATEMENT

All participants provided written informed consent before enrolment in the study, which was approved by The Ethics Committee of Affiliated Zhongda Hospital, Southeast University (2016ZDSYLL002.0 and 2016ZDSYLL002-Y01). All participants gave written informed consent in accordance

with the Declaration of Helsinki. Each participant received 200 Chinese Yuan for participating after the experiment.

AUTHOR CONTRIBUTIONS

SG conducted the experiments, data analysis and wrote the manuscript. PW, HL and PL conducted the experiments and data analysis. JG, RW and KI developed the experimental designs. QZ and WZ designed the research.

FUNDING

This work was supported in part by the National Basic Research Program of China under Grant 2015CB351704, the National

Nature Science Foundation of China (61473221, 61773408 and 61921004), and in part by the Fundamental Research Funds for the Central Universities of China (CZY18047).

ACKNOWLEDGMENTS

We thank Benjamin Knight, MSc., for editing the English text of this manuscript draft.

SUPPLEMENTARY MATERIAL

The Supplementary Material for this article can be found online at: <https://www.frontiersin.org/articles/10.3389/fnhum.2019.00357/full#supplementary-material>.

REFERENCES

- Ahn, S., and Jun, S. C. (2017). Multi-modal integration of EEG-fNIRS for brain-computer interfaces-current limitations and future directions. *Front. Hum. Neurosci.* 11:503. doi: 10.3389/fnhum.2017.00503
- Balardin, J. B., Zimeo Morais, G. A., Furucho, R. A., Trambaiolli, L., Vanzella, P., Biazoli, C., et al. (2017). Imaging brain function with functional near-infrared spectroscopy in unconstrained environments. *Front. Hum. Neurosci.* 11:258. doi: 10.3389/fnhum.2017.00258
- Bandara, D. S. V., Arata, J., and Kiguchi, K. (2018). A noninvasive brain-computer interface approach for predicting motion intention of activities of daily living tasks for an upper-limb wearable robot. *Int. J. Adv. Robot. Syst.* 15:1729881418767310. doi: 10.1177/1729881418767310
- Berger, A., Pixa, N. H., Steinberg, F., and Doppelmayr, M. (2018). Brain oscillatory and hemodynamic activity in a bimanual coordination task following transcranial alternating current stimulation (tACS): a combined EEG-fNIRS study. *Front. Behav. Neurosci.* 12:67. doi: 10.3389/fnbeh.2018.00067
- Beudt, S., and Jacobsen, T. (2015). On the role of mentalizing processes in aesthetic appreciation: an ERP study. *Front. Hum. Neurosci.* 9:600. doi: 10.3389/fnhum.2015.00600
- Boas, D. A., Dale, A. M., and Franceschini, M. A. (2004). Diffuse optical imaging of brain activation: approaches to optimizing image sensitivity, resolution and accuracy. *Neuroimage* 23, S275–S288. doi: 10.1016/j.neuroimage.2004.07.011
- Boas, D. A., Elwell, C. E., Ferrari, M., and Taga, G. (2014). Twenty years of functional near-infrared spectroscopy: introduction for the special issue. *Neuroimage* 85, 1–5. doi: 10.1016/j.neuroimage.2013.11.033
- Brown, K. S., Ortigue, S., Grafton, S. T., and Carlson, J. M. (2010). Improving human brain mapping via joint inversion of brain electrodynamics and the BOLD signal. *Neuroimage* 49, 2401–2415. doi: 10.1016/j.neuroimage.2009.10.011
- Bullmore, E. T., and Sporns, O. (2009). Complex brain networks: graph theoretical analysis of structural and functional systems. *Nat. Rev. Neurosci.* 10, 186–198. doi: 10.1038/nrn2575
- Buneo, C. A., and Andersen, R. A. (2006). The posterior parietal cortex: sensorimotor interface for the planning and online control of visually guided movements. *Neuropsychologia* 44, 2594–2606. doi: 10.1016/j.neuropsychologia.2005.10.011
- Caligiore, D., Mustile, M., Spalletta, G., and Baldassarre, G. (2017). Action observation and motor imagery for rehabilitation in Parkinson's disease: a systematic review and an integrative hypothesis. *Neurosci. Biobehav. Rev.* 72, 210–222. doi: 10.1016/j.neubiorev.2016.11.005
- Call, J., and Tomasello, M. (2008). Does the chimpanzee have a theory of mind? 30 years later. *Trends Cogn. Sci.* 12, 187–192. doi: 10.1016/j.tics.2008.02.010
- Casalino, A., Messeri, C., Pozzi, M., Zanchettin, A. M., Rocco, P., and Prattichizzo, D. (2018). Operator awareness in human-robot collaboration through wearable vibrotactile feedback. *IEEE Robot. Autom. Lett.* 3, 4289–4296. doi: 10.1109/Lra.2018.2865034
- Chang, C.-C., and Lin, C.-J. (2011). LIBSVM: a library for support vector machines. *ACM Trans. Intell. Syst. Technol.* 2:27. doi: 10.1145/1961189.1961199
- de Lange, F. P., Spronk, M., Willems, R. M., Toni, I., and Bekkering, H. (2008). Complementary systems for understanding action intentions. *Curr. Biol.* 18, 454–457. doi: 10.1016/j.cub.2008.02.057
- Delpy, D. T., Cope, M., van der Zee, P., Arridge, S., Wray, S., and Wyatt, J. (1988). Estimation of optical pathlength through tissue from direct time of flight measurement. *Phys. Med. Biol.* 33, 1433–1442. doi: 10.1088/0031-9155/33/12/008
- Eren, A. (2009). Exploring the relationships among mirror neurons, theory of mind, and achievement goals: towards a model of achievement goal contagion in educational settings. *Educ. Res. Rev.* 4, 233–247. doi: 10.1016/j.edurev.2009.03.002
- Fang, J. P., Chen, H. M., Cao, Z. T., Jiang, Y., Ma, L. Y., Ma, H. Z., et al. (2017). Impaired brain network architecture in newly diagnosed Parkinson's disease based on graph theoretical analysis. *Neurosci. Lett.* 657, 151–158. doi: 10.1016/j.neulet.2017.08.002
- Fazli, S., Mehnert, J., Steinbrink, J., Curio, G., Villringer, A., Müller, K. R., et al. (2012). Enhanced performance by a hybrid NIRS-EEG brain computer interface. *Neuroimage* 59, 519–529. doi: 10.1016/j.neuroimage.2011.07.084
- Foster, M. E., Gaschler, A., and Giuliani, M. (2017). Automatically classifying user engagement for dynamic multi-party human-robot interaction. *Int. J. Soc. Robot.* 9, 659–674. doi: 10.1007/s12369-017-0414-y
- Gardner, T., Goulden, N., and Cross, E. S. (2015). Dynamic modulation of the action observation network by movement familiarity. *J. Neurosci.* 35, 1561–1572. doi: 10.1523/JNEUROSCI.2942-14.2015
- Gatti, R., Tettamanti, A., Gough, P. M., Riboldi, E., Marinoni, L., and Buccino, G. (2013). Action observation versus motor imagery in learning a complex motor task: a short review of literature and a kinematics study. *Neurosci. Lett.* 540, 37–42. doi: 10.1016/j.neulet.2012.11.039
- Ge, S., Yang, Q., Wang, R. M., Lin, P., Gao, J. F., Leng, Y., et al. (2017). A brain-computer interface based on a few-channel EEG-fNIRS bimodal system. *IEEE Access* 5, 208–218. doi: 10.1109/ACCESS.2016.2637409
- Ge, S., Wang, R. M., and Yu, D. C. (2014). Classification of four-class motor imagery employing single-channel electroencephalography. *PLoS One* 9:e98019. doi: 10.1371/journal.pone.0098019
- Girouard, H., and Iadecola, C. (2006). Neurovascular coupling in the normal brain and in hypertension, stroke and Alzheimer disease. *J. Appl. Physiol.* 100, 328–335. doi: 10.1152/jappphysiol.00966.2005
- Govindan, R. B., Massaro, A., Chang, T., Vezina, G., and du Plessis, A. (2016). A novel technique for quantitative bedside monitoring of neurovascular coupling. *J. Neurosci. Methods* 259, 135–142. doi: 10.1016/j.jneumeth.2015.11.025
- Hamilton, A. F. D. (2015). Cognitive underpinnings of social interaction. *Q. J. Exp. Psychol. Hove* 68, 417–432. doi: 10.1080/17470218.2014.973424
- Han, C. X., Sun, X. Z., Yang, Y. R., Che, Y. Q., and Qin, Y. M. (2019). Brain complex network characteristic analysis of fatigue during

- simulated driving based on electroencephalogram signals. *Entropy* 21:353. doi: 10.3390/e21040353
- Harmsen, W. J., Bussmann, J. B., Selles, R. W., Hurkmans, H. L., and Ribbers, G. M. (2015). A mirror therapy-based action observation protocol to improve motor learning after stroke. *Neurorehabil. Neural Repair* 29, 509–516. doi: 10.1177/1545968314558598
- He, B., Yang, L., Wilke, C., and Yuan, H. (2011). Electrophysiological imaging of brain activity and connectivity-challenges and opportunities. *IEEE Trans. Biomed. Eng.* 58, 1918–1931. doi: 10.1109/tbme.2011.2139210
- Hendrikx, D., Smits, A., Lavanga, M., De Wel, O., Thewissen, L., Jansen, K., et al. (2019). Measurement of neurovascular coupling in neonates. *Front. Physiol.* 10:65. doi: 10.3389/fphys.2019.00065
- Hernandez, Z. R., Cruz-Garza, J., Tse, T., and Contreras-Vidal, J. L. (2014). “Decoding of intentional actions from scalp electroencephalography (EEG) in freely-behaving infants,” in *Proceedings of the 36th Annual International Conference of the IEEE Engineering in Medicine and Biology Society (EMBC)* (Chicago, IL, USA: IEEE), 2115–2118.
- Hong, K. S., and Khan, M. J. (2017). Hybrid brain-computer interface techniques for improved classification accuracy and increased number of commands: a review. *Front. Neurobot.* 11:35. doi: 10.3389/fnbot.2017.00035
- Iacoboni, M. (2009). Imitation, empathy, and mirror neurons. *Annu. Rev. Psychol.* 60, 653–670. doi: 10.1146/annurev.psych.60.110707.163604
- Iacoboni, M., Molnar-Szakacs, I., Gallese, V., Buccino, G., Mazziotta, J. C., and Rizzolatti, G. (2005). Grasping the intentions of others with one's own mirror neuron system. *PLoS Biol.* 3:e79. doi: 10.1371/journal.pbio.0030079
- Jelone-Swain, L., Persad, C., Burkard, D., and Welsh, R. C. (2015). Action processing and mirror neuron function in patients with amyotrophic lateral sclerosis: an fMRI study. *PLoS One* 10:e0119862. doi: 10.1371/journal.pone.0119862
- Jeon, H., and Lee, S. H. (2018). From neurons to social beings: short review of the mirror neuron system research and its socio-psychological and psychiatric implications. *Clin. Psychopharmacol. Neurosci.* 16, 18–31. doi: 10.9758/cpn.2018.16.1.18
- Kamran, M. A., Mannan, M. M. N., and Jeong, M. Y. (2016). Cortical signal analysis and advances in functional near-infrared spectroscopy signal: a review. *Front. Hum. Neurosci.* 10:261. doi: 10.3389/fnhum.2016.00261
- Kanokogi, Y., and Itakura, S. (2010). The link between perception and action in early infancy: from the viewpoint of the direct-matching hypothesis. *Jpn. Psychol. Res.* 52, 121–131. doi: 10.1111/j.1468-5884.2010.00429.x
- Keeser, D., Padberg, F., Reisinger, E., Pogarell, O., Kirsch, V., Palm, U., et al. (2011). Prefrontal direct current stimulation modulates resting EEG and event-related potentials in healthy subjects: a standardized low resolution tomography (sLORETA) study. *Neuroimage* 55, 644–657. doi: 10.1016/j.neuroimage.2010.12.004
- Keles, H. O., Barbour, R. L., and Omurtag, A. (2016). Hemodynamic correlates of spontaneous neural activity measured by human whole-head resting state EEG plus fNIRS. *Neuroimage* 138, 76–87. doi: 10.1016/j.neuroimage.2016.05.058
- Khan, M. J., and Hong, K. S. (2017). Hybrid EEG-fNIRS-based eight-command decoding for BCI: application to quadcopter control. *Front. Neurobot.* 11:6. doi: 10.3389/fnbot.2017.00006
- Kilner, J. M. (2011). More than one pathway to action understanding. *Trends Cogn. Sci.* 15, 352–357. doi: 10.1016/j.tics.2011.06.005
- Kim, T., Frank, C., and Schack, T. (2017). A systematic investigation of the effect of action observation training and motor imagery training on the development of mental representation structure and skill performance. *Front. Hum. Neurosci.* 11:499. doi: 10.3389/fnhum.2017.00499
- Kononenko, I. (1994). “Estimating attributes: analysis and extensions of RELIEF,” in *European Conference on Machine Learning on Machine Learning*, eds F. Bergadano and L. De Raedt (Berlin: Springer), 171–182.
- Lamm, C., Windischberger, C., Moser, E., and Bauer, H. (2007). The functional role of dorso-lateral premotor cortex during mental rotation. An event-related fMRI study separating cognitive processing steps using a novel task paradigm. *Neuroimage* 36, 1374–1386. doi: 10.1016/j.neuroimage.2007.04.012
- Lee, S. Y., Bae, S. S., Han, J. T., Byun, S. D., and Chang, J. S. (2012). The effect of motor learning of serial reaction time task (SRTT) through action observation on mu rhythm and improvement of behavior abilities. *J. Clin. Med. Res.* 4, 114–118. doi: 10.4021/jocmr727w
- Liang, Y., Liu, B., Li, X., and Wang, P. (2018). Multivariate pattern classification of facial expressions based on large-scale functional connectivity. *Front. Hum. Neurosci.* 12:94. doi: 10.3389/fnhum.2018.00094
- Libero, L. E., Maximo, J. O., Deshpande, H. D., Klinger, L. G., Klinger, M. R., and Kana, R. K. (2014). The role of mirroring and mentalizing networks in mediating action intentions in autism. *Mol. Autism* 5:50. doi: 10.1186/2040-2392-5-50
- Lin, S. H., Keysar, B., and Epley, N. (2010). Reflexively mindblind: using theory of mind to interpret behavior requires effortful attention. *J. Exp. Soc. Psychol.* 46, 551–556. doi: 10.1016/j.jesp.2009.12.019
- Matthys, K., Smits, M., Van Der Geest, J. N., Van der Lugt, A., Seurinck, R., Stam, H. J., et al. (2009). Mirror-induced visual illusion of hand movements: a functional magnetic resonance imaging study. *Arch. Phys. Med. Rehabil.* 90, 675–681. doi: 10.1016/j.apmr.2008.09.571
- Mohring, N., Brandt, E. S. L., Mohr, B., Pulvermuller, F., and Neuhaus, A. H. (2014). ERP adaptation provides direct evidence for early mirror neuron activation in the inferior parietal lobule. *Int. J. Psychophysiol.* 94, 76–83. doi: 10.1016/j.ijpsycho.2014.07.001
- Molenberghs, P., Cunnington, R., and Mattingley, J. B. (2012). Brain regions with mirror properties: a meta-analysis of 125 human fMRI studies. *Neurosci. Biobehav. Rev.* 36, 341–349. doi: 10.1016/j.neubiorev.2011.07.004
- Oh, H., Braun, A. R., Reggia, J. A., and Gentili, R. J. (2019). Fronto-parietal mirror neuron system modeling: visuospatial transformations support imitation learning independently of imitator perspective. *Hum. Mov. Sci.* 65, 121–141. doi: 10.1016/j.humov.2018.05.013
- Ortigue, S., Sinigaglia, C., Rizzolatti, G., and Grafton, S. T. (2010). Understanding actions of others: the electrodynamics of the left and right hemispheres. A high-density EEG neuroimaging study. *PLoS One* 5:e12160. doi: 10.1371/journal.pone.0012160
- Ortigue, S., Thompson, J. C., Parasuraman, R., and Grafton, S. T. (2009). Spatio-temporal dynamics of human intention understanding in temporo-parietal cortex: a combined EEG/fMRI repetition suppression paradigm. *PLoS One* 4:e6962. doi: 10.1371/journal.pone.0006962
- Pascual-Marqui, R. D. (2002). Standardized low-resolution brain electromagnetic tomography (sLORETA): technical details. *Methods Find. Exp. Clin. Pharmacol.* 24, 5–12. doi: 10.1358/mf.2002.24.1.677125
- Pascual-Marqui, R. D., Esslen, M., Kochi, K., and Lehmann, D. (2002). Functional imaging with low-resolution brain electromagnetic tomography (LORETA): a review. *Methods Find. Exp. Clin. Pharmacol.* 24, 91–95. doi: 10.1002/med.10000
- Perkins, T. J., Bittar, R. G., McGillivray, J. A., Cox, I. L., and Stokes, M. A. (2015). Increased premotor cortex activation in high functioning autism during action observation. *J. Clin. Neurosci.* 22, 664–669. doi: 10.1016/j.jocn.2014.10.007
- Pfurtscheller, G., Daly, I., Bauernfeind, G., and Müller-Putz, G. R. (2012). Coupling between intrinsic prefrontal HbO₂ and central EEG beta power oscillations in the resting brain. *PLoS One* 7:e43640. doi: 10.1371/journal.pone.0043640
- Putze, F., Hesslering, S., Tse, C. Y., Huang, Y., Herff, C., Guan, C., et al. (2014). Hybrid fNIRS-EEG based classification of auditory and visual perception processes. *Front. Neurosci.* 8:373. doi: 10.3389/fnins.2014.00373
- Reader, A. T., Royce, B. P., Marsh, J. E., Chivers, K. J., and Holmes, N. P. (2018). Repetitive transcranial magnetic stimulation reveals a role for the left inferior parietal lobule in matching observed kinematics during imitation. *Eur. J. Neurosci.* 47, 918–928. doi: 10.1111/ejn.13886
- Rilling, J. K., Sanfey, A. G., Aronson, J. A., Nystrom, L. E., and Cohen, J. D. (2004). The neural correlates of theory of mind within interpersonal interactions. *Neuroimage* 22, 1694–1703. doi: 10.1016/j.neuroimage.2004.04.015
- Rizzolatti, G., Cattaneo, L., Fabbri-Destro, M., and Rozzi, S. (2014). Cortical mechanisms underlying the organization of goal-directed actions and mirror neuron-based action understanding. *Physiol. Rev.* 94, 655–706. doi: 10.1152/physrev.00009.2013
- Rizzolatti, G., and Craighero, L. (2004). The mirror-neuron system. *Annu. Rev. Neurosci.* 27, 169–192. doi: 10.1146/annurev.neuro.27.070203.144230
- Rizzolatti, G., Fogassi, L., and Gallese, V. (2001). Neurophysiological mechanisms underlying the understanding and imitation of action. *Nat. Rev. Neurosci.* 2, 661–670. doi: 10.1038/35090060
- Santiago, E., Velasco-Hernandez, J. X., and Romero-Salcedo, M. (2016). A descriptive study of fracture networks in rocks using complex network metrics. *Comput. Geosci.* 88, 97–114. doi: 10.1016/j.cageo.2015.12.021

- Schultz, J., Imamizu, H., Kawato, M., and Frith, C. D. (2004). Activation of the human superior temporal gyrus during observation of goal attribution by intentional objects. *J. Cogn. Neurosci.* 16, 1695–1705. doi: 10.1162/0898929042947874
- Shon, S. H., Yoon, W., Kim, H., Joo, S. W., Kim, Y., and Lee, J. (2018). Deterioration in global organization of structural brain networks in schizophrenia: a diffusion MRI tractography study. *Front. Psychiatry* 9:272. doi: 10.3389/fpsy.2018.00272
- Sood, M., Besson, P., Muthalib, M., Jindal, U., Perrey, S., Dutta, A., et al. (2016). NIRS-EEG joint imaging during transcranial direct current stimulation: online parameter estimation with an autoregressive model. *J. Neurosci. Methods* 274, 71–80. doi: 10.1016/j.jneumeth.2016.09.008
- Sporns, O. (2013). Structure and function of complex brain networks. *Dialogues Clin. Neurosci.* 15, 247–262.
- Spunt, R. P., Falk, E. B., and Lieberman, M. D. (2010). Dissociable neural systems support retrieval of how and why action knowledge. *Psychol. Sci.* 21, 1593–1598. doi: 10.1177/0956797610386618
- Spunt, R. P., Satpute, A. B., and Lieberman, M. D. (2011). Identifying the what, why, and how of an observed action: an fMRI study of mentalizing and mechanizing during action observation. *J. Cogn. Neurosci.* 23, 63–74. doi: 10.1162/jocn.2010.21446
- Talairach, J., and Tournoux, P. (1988). *Co-Planar Stereotaxic Atlas of the Human Brain: 3-Dimensional Proportional System: An Approach to Cerebral Imaging*. Stuttgart; New York, NY: Georg Thieme.
- Thioux, M., Gazzola, V., and Keysers, C. (2008). Action understanding: how, what and why. *Curr. Biol.* 18, R431–R434. doi: 10.1016/j.cub.2008.03.018
- Umiltà, M. A., Kohler, E., Gallese, V., Fogassi, L., Fadiga, L., Keysers, C., et al. (2001). I know what you are doing: a neurophysiological study. *Neuron* 31, 155–165. doi: 10.1016/s0896-6273(01)00337-3
- van Overwalle, F., and Baetens, K. (2009). Understanding others' actions and goals by mirror and mentalizing systems: a meta-analysis. *Neuroimage* 48, 564–584. doi: 10.1016/j.neuroimage.2009.06.009
- Villringer, A., and Chance, B. (1997). Non-invasive optical spectroscopy and imaging of human brain function. *Trends Neurosci.* 20, 435–442. doi: 10.1016/s0166-2236(97)01132-6
- World Medical Association. (2013). World medical association declaration of Helsinki: ethical principles for medical research involving human subjects. *JAMA* 310, 2191–2194. doi: 10.1001/jama.2013.281053
- Yang, D. Y. J., Rosenblau, G., Keifer, C., and Pelphrey, K. A. (2015). An integrative neural model of social perception, action observation, and theory of mind. *Neurosci. Biobehav. Rev.* 51, 263–275. doi: 10.1016/j.neubiorev.2015.01.020
- Yu, P. S., Chen, S. T., and Chang, I. F. (2006). Support vector regression for real-time flood stage forecasting. *J. Hydrol.* 328, 704–716. doi: 10.1016/j.jhydrol.2006.01.021
- Yu, Q., Du, Y., Chen, J., Sui, J., Adali, T., Pearlson, G. D., et al. (2018). Application of graph theory to assess static and dynamic brain connectivity: approaches for building brain graphs. *Proc. IEEE Inst. Electr. Electron. Eng.* 106, 886–906. doi: 10.1109/jproc.2018.2825200
- Zhang, L., Gan, J. Q., Zheng, W. M., and Wang, H. X. (2018). Spatiotemporal phase synchronization in adaptive reconfiguration from action observation network to mentalizing network for understanding other's action intention. *Brain Topogr.* 31, 447–467. doi: 10.1007/s10548-017-0614-7
- Zhang, J., Li, Y., Chen, H., Ding, J., and Yuan, Z. (2016). An investigation of the differences and similarities between generated small-world networks for right- and left-hand motor imageries. *Sci. Rep.* 6:36562. doi: 10.1038/srep36562
- Zhang, Z., Yang, Q., Leng, Y., Yang, Y. K., and Ge, S. (2015). "Classification of intention understanding using EEG-NIRS bimodal system," in *Proceedings of the 12th International Computer Conference on Wavelet Active Media Technology and Information Processing (ICCWAMTIP)* (Chengdu, China: IEEE), 67–70.
- Zhao, C., Zhao, M., Yang, Y., Gao, J. F., Rao, N., and Lin, P. (2017). The reorganization of human brain networks modulated by driving mental fatigue. *IEEE J. Biomed. Health Inform.* 21, 743–755. doi: 10.1109/jbhi.2016.2544061

Conflict of Interest: The authors declare that the research was conducted in the absence of any commercial or financial relationships that could be construed as a potential conflict of interest.

The handling editor is currently co-organizing a Research Topic with one of the reviewers ZY, and confirms the absence of any other collaboration.

Copyright © 2019 Ge, Wang, Liu, Lin, Gao, Wang, Iramina, Zhang and Zheng. This is an open-access article distributed under the terms of the Creative Commons Attribution License (CC BY). The use, distribution or reproduction in other forums is permitted, provided the original author(s) and the copyright owner(s) are credited and that the original publication in this journal is cited, in accordance with accepted academic practice. No use, distribution or reproduction is permitted which does not comply with these terms.